

Bottlebrush Glycopolymers from 2-Oxazolines and Acrylamides for Targeting Dendritic Cell-Specific Intercellular Adhesion Molecule-3-Grabbing Nonintegrin and Mannose-Binding Lectin

Valentin P. Beyer, Alessandra Monaco, Richard Napier, Gokhan Yilmaz, and C. Remzi Becer*

Cite This: *Biomacromolecules* 2020, 21, 2298–2308

Read Online

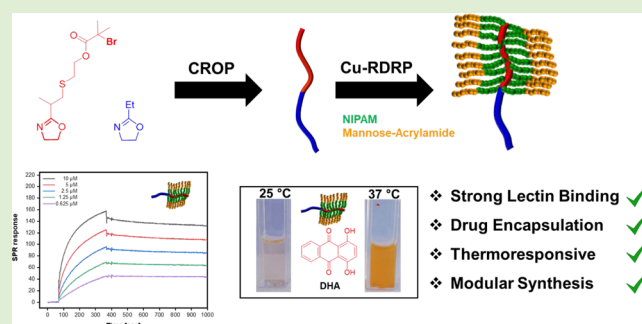
ACCESS |

Metrics & More

Article Recommendations

Supporting Information

ABSTRACT: Lectins are omnipresent carbohydrate binding proteins that are involved in a multitude of biological processes. Unearthing their binding properties is a powerful tool toward the understanding and modification of their functions in biological applications. Herein, we present the synthesis of glycopolymers with a brush architecture via a “grafting from” methodology. The use of a versatile 2-oxazoline inimer was demonstrated to open avenues for a wide range of 2-oxazoline/acrylamide bottle brush polymers utilizing aqueous Cu-mediated reversible deactivation radical polymerization (Cu-RDRP). The polymers in the obtained library were assessed for their thermal properties in aqueous solution and their binding toward the C-type animal lectins dendritic cell-specific intercellular adhesion molecule-3-grabbing nonintegrin (DC-SIGN) and mannose-binding lectin (MBL) via surface plasmon resonance spectrometry. The encapsulation properties of a hydrophobic drug-mimicking compound demonstrated the potential use of glyco brush copolymers in biological applications.



INTRODUCTION

Carbohydrate-binding proteins, also known as lectins, are found across the plant and animal kingdom, encompassing a myriad of crucial biological functions, such as immune response, inflammatory response, cell signaling, and cell growth, among others.^{1,2} Interactions between lectins and carbohydrate units of glycan ligands are weak. However, binding affinity is achieved by the multivalent nature of the protein and the resulting “glycocluster effect” in combination with the sugar density of the ligand.^{3,4} The binding behavior of carbohydrate-binding proteins is of particular interest because cancer cells and other pathogens show alterations in the typical glycosylation patterns on the cell surface (glycocalyx). These abnormalities in the glycocalyx can be targeted by certain lectins, paving the way for lectin-based diagnostics and therapies.^{5–8} Furthermore, multiple lectins are known to interact with a number of viruses, making them promising targets for the treatment and prevention of viral infections.^{9,10} Dendritic cell-specific intercellular adhesion molecule-3-grabbing nonintegrin (DC-SIGN) and mannose-binding lectin (MBL) are the subjects of extensive research due to their key role in pathogen response after viral infections, including HIV.^{11–15} The tetrameric structure of DC-SIGN leads to great selectivity toward mannose- and/or fucose-containing glycopolymers.¹⁶ Furthermore, MBL was found to play an important role in the immunological defense by binding to numerous parasites, viruses, and bacteria, such as *Neisseria meningitidis*,

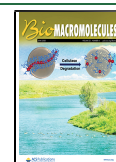
Ebola, and *Influenza A*.^{17–20} MBL is presenting different structural forms ranging from dimers to hexamers based on oligomers exhibiting three peptide chains with a carbohydrate-recognition domain, which binds to multiple sugars and glycopolymers with high affinities.²¹

Therefore, synthetic lectin ligands in the form of glycopolymers emerged to be essential components in the development of an in-depth understanding of lectin–glycan interactions.²² The development and optimization of “living” polymerization techniques enables the synthesis of glycopolymers comprising a wide range of monomers and architectures. In combination with the powerful tool of “click chemistry”, these parameters are easily adjusted, allowing the versatile synthesis of tailor-made macromolecules to investigate the host–guest interaction of lectins with carbohydrates.^{23,24} There have been numerous reports for the synthesis of lectin-binding glycopolymers, encompassing linear polymers,^{11,25–31} glyconanoparticles,^{32–39} hyperbranched architectures,^{40–43} star polymers,^{44–47} and dendrimers.^{48–50} Furthermore, various sugar-containing copolymers from *N*-(2-

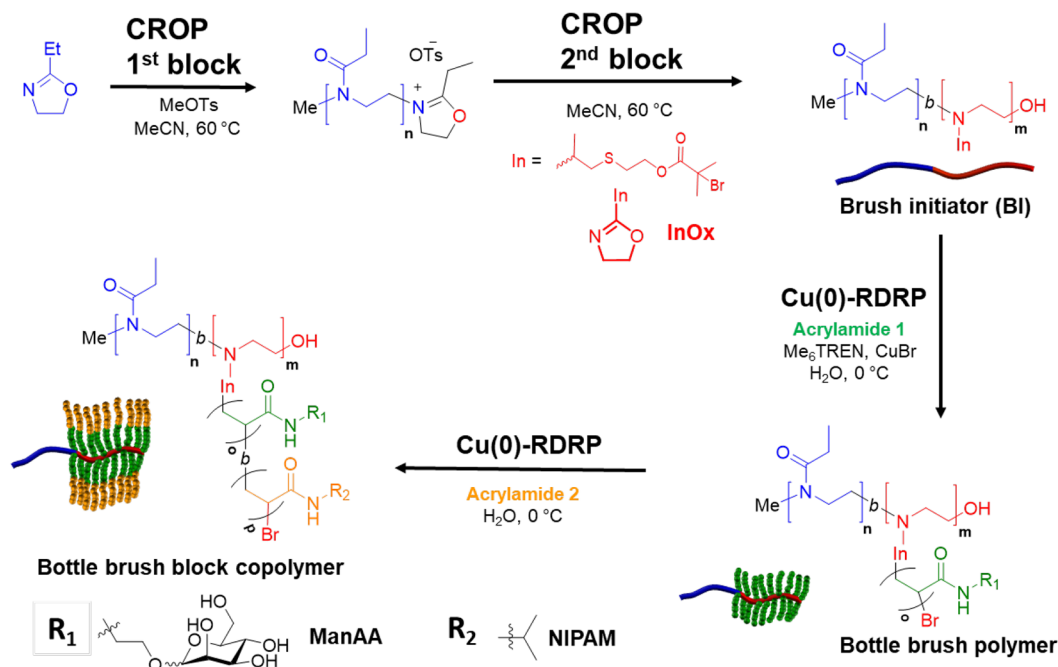
Received: February 19, 2020

Revised: April 21, 2020

Published: April 22, 2020



Scheme 1. Schematic Representation of the Synthetic Pathway of Glyco Brush Copolymers Based on 2-Oxazolines and Acrylamides by Cationic Ring-Opening Polymerization (CROP) (yielding brush initiator BI) and Subsequent Cu-Mediated RDRP of Acrylamides (yielding brush copolymers)



hydroxypropyl)methacrylamide (HPMA) have been employed to study polymer–lectin interactions.^{51–55} In order to accelerate the lectin binding, a high sugar density is favorable to drive the “glycocluster effect”; therefore, branched structures and graft polymers allow faster kinetics for protein binding.⁵⁶ Surprisingly, there are only a few examples demonstrating the lectin-binding of glyco brush polymers, and they mainly comprise surface-grafted architectures.^{57,58}

Poly(2-oxazolines) are a class of biocompatible polymers that are gaining growing attention due to their unique physicochemical properties and stealth behavior, outperforming the gold-standard polyethylene glycol (PEG).^{59–65} However, there have been only a few reports in the literature synthesizing sugar-containing poly(2-oxazolines).^{66–68} To the best of our knowledge, bottlebrush glycopolymers consisting of a poly(2-oxazoline) backbone and polyacrylamide brushes have not been synthesized to date. The peptidomimetic backbone of poly(2-oxazolines) equips the materials with a biocompatible feature, and the chemical composition yields brush copolymers with polymer chains grafted from every third backbone atom. Contrarily, a poly(acrylate) pendant would offer grafted polymer chains from every second backbone atom.

In this work, we demonstrate a versatile approach toward thermoresponsive glycopolymer brushes by grafting acrylamides from a functional poly(2-oxazoline) inimer (InOx) backbone (Scheme 1). Combined with aqueous Cu-mediated reversible deactivation radical polymerization (Cu-RDRP), glycopolymers with random- or block-polyacrylamide brushes consisting of *N*-isopropylacrylamide (NIPAM) and 2-(*D*-manosyloxy) hydroxyethylacrylamide (ManAA) are rapidly synthesized, and their lectin interactions with the C-type lectins DC-SIGN and MBL were assessed. Furthermore, the potential use of these brush copolymers for drug delivery purposes was assessed by measuring the encapsulation of a hydrophobic small molecule via UV–vis measurements. By

varying the amount of NIPAM and its distribution within the polymers, the thermoresponsive behavior was shown to vary, allowing one to control the solution behavior and therefore the polymer properties in terms of encapsulation and particle size.

EXPERIMENTAL SECTION

Instruments. Nuclear Magnetic Resonance. Nuclear magnetic resonance spectra were recorded on a Bruker AV-III at 400 MHz for ¹H and at 100 MHz for ¹³C NMR measurements. CDCl₃ was used as solvent, and the resonance signal of residual CHCl₃ at 7.26 ppm (¹H) and 77.16 ppm (¹³C) served as the reference for the chemical shift, δ . For DMSO-*d*₆, the resonance signal of residual DMSO at 2.50 ppm (¹H) was used. For D₂O, the resonance signal of water at 4.79 ppm (¹H) was used.

Size Exclusion Chromatography (SEC) in DMF. SEC measurements were conducted on an Agilent 1260 Infinity system operating in DMF with 5 mM NH₄BF₄ and equipped with refractive index and variable wavelength detectors, two PLgel 5 μ m mixed-C columns (300 \times 7.5 mm), a PLgel 5 mm guard column (50 \times 7.5 mm), and an autosampler. The instrument was calibrated with linear, narrow PMMA standards. All samples were filtered through 0.2 μ m Nylon filters before analysis.

Surface Plasmon Resonance (SPR). SPR was used for interaction analysis of DC-SIGN and MBL. The extent of interaction between the glycopolymers and lectins was evaluated on a BIAcore 2000 system (GE Healthcare). DC-SIGN and MBL (0.005 mg/mL) were immobilized via a standard amino-coupling protocol onto a CM5 sensor chip that was activated by flowing a 1/1 mixture of 0.1 M *N*-hydroxysuccinimide and 0.1 M *N*-ethyl-*N'*-(dimethylaminopropyl)-carbodiimide over the chip for 5 min at 25 °C at a flow rate of 5 μ L/min. Immobilization of lectins was targeted to 3000 response units (RU⁻¹), in order to ensure a fair comparison between MBL and DC-SIGN. Subsequently, all channels were blocked with ethanolamine (1 M pH 8.5) for 10 min at 5 μ L/min to remove remaining reactive groups. All experiments were conducted with HEPES-buffered saline (HBS) (0.10 M HEPES, 0.9 M NaCl, 1 mM MgCl₂, 1 mM CaCl₂, 1 mM MnCl₂, 0.01% P20 surfactant solution adjusted to pH 7.4) and filtered using a 0.2 μ m regenerated cellulose syringe filter. Sensor

Table 1. Summary of SEC Results, Turbidity, and DLS Results for the Synthesized Polymer Library

code	monomer and DP	SEC results			cloud point ^a (°C)		DLS in H ₂ O ^c Z-average diameter (nm)	
		$M_{n,theo}$ (Da)	$M_{n,SEC}$ (Da)	\bar{D}	H ₂ O	HBS ^b	25 °C	37 °C
Linear Arms Architecture								
L1	NIPAM ₁₀ - <i>b</i> -ManAA ₁₀	4 100	10 700	1.10	–	–	nd	nd
L2	NIPAM ₅₀ - <i>b</i> -ManAA ₁₀	8 400	13 000	1.10	–	–	nd	nd
L3	NIPAM ₁₀ - <i>r</i> -ManAA ₁₀	4 100	16 400	1.42	–	–	nd	nd
L4	NIPAM ₅₀ - <i>r</i> -ManAA ₁₀	8 400	16 700	2.52	–	47	nd	nd
Brush Initiator Architecture								
BI	EtOx ₄₀ - <i>b</i> -InOx ₁₀	7 500	11 100	1.11	70	nd	nd	nd
Brush Homo Architecture								
BP1	NIPAM ₁₀	18 700	22 000	1.38	–	nd	14	24
BP2	NIPAM ₅₀	63 900	84 000	1.50	36	nd	19	189
BP3	ManAA ₁₀	35 200	16 400	1.38	–	–	45	74
BP4	ManAA ₂₅	76 800	18 100	1.44	–	–	50	57
Brush Random Architecture								
BP5	NIPAM ₁₀ - <i>r</i> -ManAA ₁₀	46 500	276 200	1.85	–	–	42	42
BP6	NIPAM ₅₀ - <i>r</i> -ManAA ₁₀	91 700	88 700	1.66	68	48	24	36
Brush Block Architecture								
BP7	NIPAM ₁₀ - <i>b</i> -ManAA ₁	21 600	28 500	1.23	66	48	14	25
BP8	NIPAM ₁₀ - <i>b</i> -ManAA ₁₀	46 500	27 900	1.52	–	–	14	25
BP9	NIPAM ₅₀ - <i>b</i> -ManAA ₁	66 800	89 600	2.28	37	21	30	221
BP10	NIPAM ₅₀ - <i>b</i> -ManAA ₁₀	91 700	79 800	1.67	–	–	33	74
BP11	ManAA ₁₀ - <i>b</i> -NIPAM ₁₀	46 500	35 700	1.24	–	–	33	30
BP12	ManAA ₁₀ - <i>b</i> -NIPAM ₅₀	91 700	97 900	1.42	–	29	25	52

^aCloud points were measured at 500 nm and values were determined at a transmission of 50%; polymer concentrations in water and HBS buffer were at 30 μM. nd = not determined. ^bHEPES-buffered saline (10 mM HEPES pH 7.4, 150 mM NaCl, 5 mM CaCl₂) (HBS). ^cPolymer concentration for the solutions was set at 1 mg/mL.

grams for each glycopolymer concentration (0.0625–10 μM) were recorded using a 300 s on period, followed by 600 s of buffer alone (off period). Regeneration of the sensor chip surfaces was performed using 10 mM HEPES (pH 7.4), 150 mM NaCl, 10 mM EDTA, and 0.01% P20 surfactant solution. Kinetic data were evaluated using a single set of sites (1/1 Langmuir binding) model.

Dynamic Light Scattering (DLS). The mean hydrodynamic diameters (the volume weight diameter of the distribution) were determined by using a Malvern Zetasizer Nano ZS instrument equipped with a He–Ne laser at 633 nm. DLS measurements were performed by taking 1 mL of polymer solution (1 mg/mL). All measurements were carried out from 25 to 40 °C and repeated three times.

UV–Vis Measurements. UV–vis measurements were carried out on an Agilent Cary 100 UV–vis instrument. Solutions were measured using quartz cuvettes for organic solvents or high temperatures and in disposable plastic cuvettes for aqueous solutions. For turbidity measurements, the absorbance at 500 nm was determined over the desired temperature range.

DHA Uptake Measurement. To a vial with a magnetic follower were added 3 mL of glycopolymer solution (1 mg/mL) and excess DHA (15 mg). The mixture was vigorously stirred for 12 h under ambient temperature or 37 °C and then passed through a 0.45 μm filter to remove any insoluble DHA. The obtained clear solution was directly used for UV–vis measurements. The absorbance was measured at 485 nm. Due to the insolubility of DHA in water, a calibration line could not be created. Therefore, the encapsulated amounts were not quantified.

Synthesis and Characterization. One-Pot Synthesis of 2-Oxazoline Inimer InOx via Mercaptoethanol Thiol–Ene Reaction and Subsequent DIC-Coupling with Bromoisobutyric Acid. Under an argon atmosphere, 2-isopropenyl-2-oxazoline (1.00 equiv) and 2-mercaptoethanol (1.00 equiv) were stirred for 15 min in a round-bottom flask. The reaction mixture was then diluted with anhydrous DCM before addition of DMAP (0.10 equiv) and α-bromoisobutyric acid (1.00 equiv). In a dropping funnel, a solution of N_iN′-

diisopropylcarbodiimide (1.00 equiv) in DCM was added slowly to the ice-cold reaction mixture. After 18 h, the formed urea byproduct was filtered off and the crude product was washed with NaHCO₃ (3×) and brine. Evaporation of the solvents under reduced pressure yielded a yellow oil that was subjected to flash chromatography on silica (ethyl acetate/hexanes = 1:9) to obtain the product as a colorless oil (yield = 61–68%).

General Procedure for the Synthesis of Brush Initiator BI: CROP of Poly(EtOx₄₀-*b*-InOx₁₀). Under an inert atmosphere, a glass vial was loaded with the monomer EtOx (40 equiv), MeOTs (1.00 equiv), and MeCN to obtain a monomer concentration of 4 M. The reaction mixture was degassed at ambient temperature for 30 min and placed in a preheated oil bath at 60 °C. After full monomer conversion, a 4 M solution of InOx (10 equiv) in MeCN was added via a degassed syringe and the reaction mixture was allowed to stir until full monomer conversion was observed.

Subsequently, 2 mL of water was added to quench the reaction and the reaction mixture was allowed to stir for 2 h. The obtained crude was placed in a dialysis membrane and dialysis was carried out against deionized water. After freeze-drying, the pure block copolymer was obtained as a white powder and was analyzed by SEC (DMF + 5 mM NH₄BF₄) and ¹H NMR.

General Procedure for the Synthesis of Brush Polymers via Cu(0)-RDRP with Chain Extension Using Brush Initiator BI. In a glass vial, Me₆TREN (0.40 equiv) was mixed with 2 mL of deionized water and degassed at 0 °C for 20 min. The solution was added to a second vial containing CuBr (0.40 equiv) and a magnetic follower via a gastight syringe at 0 °C. In the meantime, another glass vial with the brush initiator BI (1.00 equiv, calculated from the molecular weight of the monomer unit) and the first monomer (desired degree of polymerization) dissolved in 2 mL of H₂O was purged with nitrogen at 0 °C. In order to start the polymerization, the monomer/initiator solution was transferred in a gastight syringe to the glass vial containing the disproportionate copper/ligand suspension. For random copolymers from two different monomers, both monomers were dissolved in one glass vial. In order to conduct chain extension

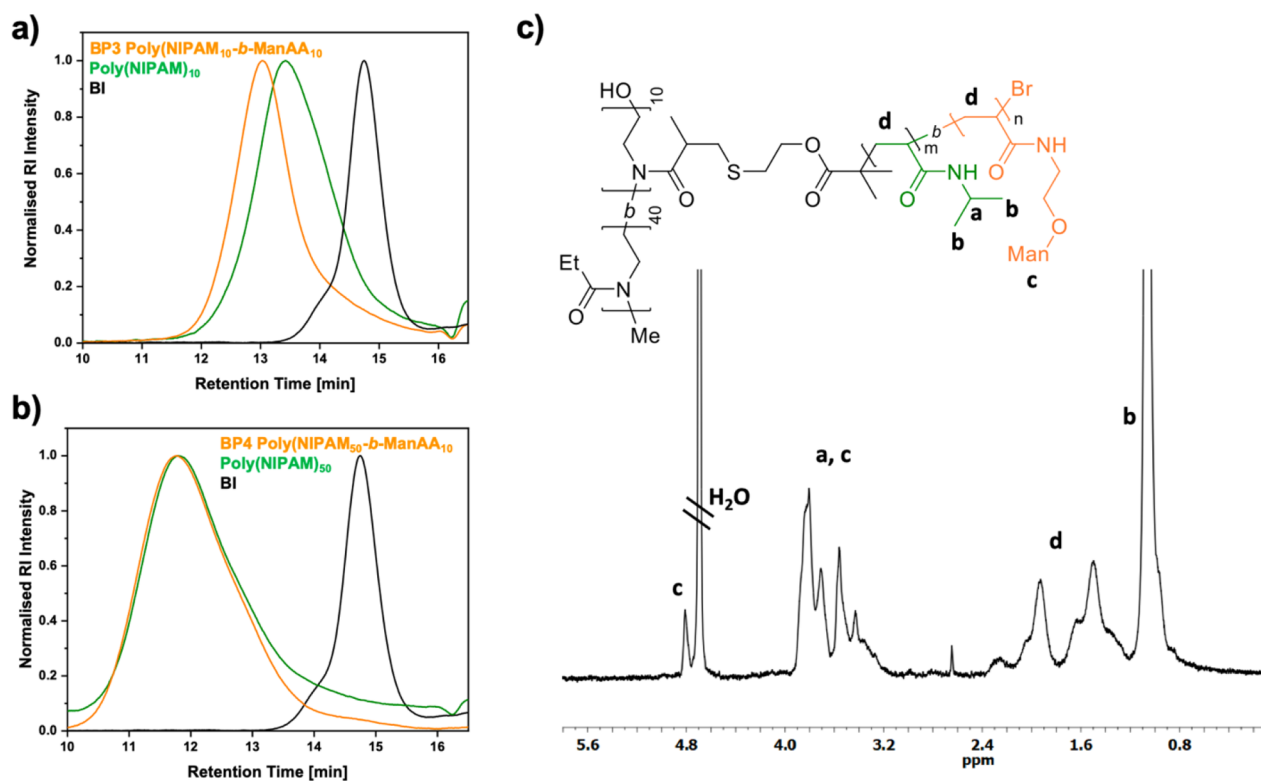


Figure 1. Size exclusion chromatography (SEC) traces of glyco brush copolymers BP3 (a) and BP4 (b), including 2-oxazoline-based brush initiator BI (black traces). (c) A representative ^1H NMR spectrum of a glycol brush copolymer BP3 showing resonances of both monomers.

experiments, the second monomer (desired degree of polymerization) was dissolved in 2 mL of deionized water and degassed with nitrogen at 0 °C. After full monomer conversion for the first block (confirmed by ^1H NMR), the degassed solution of the second monomer was added to the polymerization reaction. The reaction was monitored by SEC (DMF with 5 mM NH_4BF_4) and ^1H NMR, and after full monomer conversion, the reaction mixture was filtered over cotton wool followed by dialysis against deionized water. The pure polymers were obtained as white powders upon freeze-drying of the dialyzed solution.

RESULTS AND DISCUSSION

Synthesis and Characterization of Glyco Brush Copolymers. With the intention to synthesize glycopolymer brushes densely decorated with carbohydrates, our very recently reported 2-oxazoline inimer approach was employed to tailor mannose-containing bottlebrushes.⁶⁹ In order to obtain a water-soluble oxazoline brush initiator BI, the α -bromoisobutyric acid containing 2-oxazoline inimer (InOx, DP = 10), which is equipped with a tertiary alkyl bromide function, was copolymerized via CROP with 2-ethyl-2-oxazoline (EtOx, DP = 40) to yield a well-defined diblock copolymer (\bar{D} = 1.11, $M_{n,\text{SEC}}$ = 11 100 Da). The water-soluble macroinitiator BI was utilized in aqueous Cu-mediated RDRP to synthesize a library of bottlebrush polymers with different monomer compositions. The monomers of choice were 2-(*D*-manosyloxy) hydroxyethylacrylamide (ManAA) for the interaction with mannose-binding lectins and NIPAM in order to introduce thermoresponsiveness. Employing a thermoresponsive monomer allows one to modulate the solution behavior of the synthesized polymers, which is a useful tool for possible applications in drug delivery and protein interaction, among others. The polymer library comprised brushes of NIPAM only (BP1 and

BP2, DP = 10 and 50, respectively) as control polymers, ManAA only (BP3 and BP4, DP = 10 and 25, respectively), and copolymer brushes of different ratios of NIPAM and ManAA consisting of random or block monomer sequences (Table 1). An identical synthesis protocol was followed for the synthesis of all brush copolymers, utilizing water as a solvent, Me_6TREN as a ligand, and CuBr as the copper source. In a conventional reaction setup, reactant ratios were maintained at $[\text{monomer}]/[\text{initiator}]/[\text{Me}_6\text{TREN}]/[\text{CuBr}] = \text{DP}/1/0.40/0.40$. Block polymer brushes were synthesized via sequential monomer addition after full conversion of the first segment. Linear control polymers with the same composition as the polymer brushes were synthesized with the same reaction procedure, utilizing 2,3-dihydroxypropyl-2-bromo-2-methylpropanoate as the monofunctional initiator (L1–L4). For all synthesized polymers, quantitative monomer conversions were obtained.

Molecular weight distributions (\bar{D}) were relatively low for brush polymers consisting of only NIPAM or brush block copolymers from NIPAM and ManAA, when low degrees of polymerization (DP) were targeted (\bar{D} = 1.21–1.52), and elevated for block copolymer brushes with higher degrees of polymerization (\bar{D} = 1.50–2.28). Nonsymmetrical SEC traces with high molecular weight shoulders and therefore high molecular weight distributions were obtained for random copolymers in general, when equal amounts of NIPAM and ManAA were copolymerized (\bar{D} = 1.66–1.85). This trend was confirmed by the random copolymerization of linear NIPAM and ManAA (L3, L4), which led to increased polydispersity values (\bar{D} = 1.42–2.52). Contrarily, linear block copolymers from NIPAM and ManAA (L1, L2) resulted in well-defined macromolecules (\bar{D} = 1.10). The generally increased \bar{D} is explained by the rapid polymerization kinetics and the fact

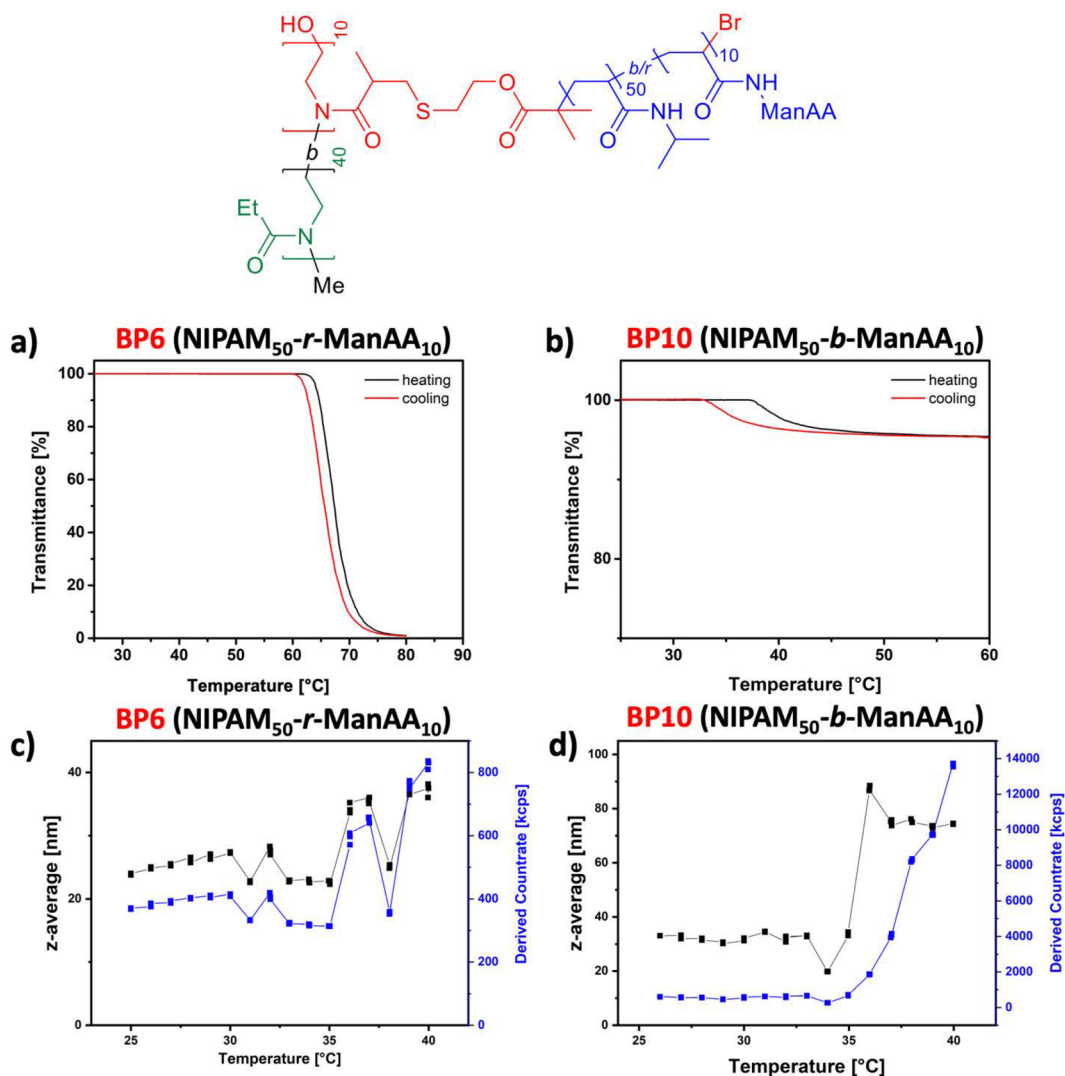


Figure 2. UV–vis spectroscopy measurements of aqueous solutions from brush polymers consisting of brushes with 50 NIPAM units and 10 ManAA units: (a) random monomer distribution (BP6) and (b) block copolymer (BP10). DLS measurements for a temperature range from 25 to 40 °C: (c) random monomer distribution (BP6) and (d) block copolymer (BP10).

that, during brush polymer synthesis, initiating sites and growing chains are in close proximity to one another, which might result in termination by combination. The decreased control for random copolymers is thought to result from the different propagation rates of NIPAM (polymerizing fast) and ManAA (polymerizing slow) [Figure S4, Supporting Information (SI)]. The successful chain extension experiments were confirmed by ¹H NMR and SEC measurements (Table 1). The clear shift of SEC traces was observed when NIPAM and ManAA were polymerized in equal amounts (both DP = 10, BP3). In the case of higher NIPAM content (DP = 50), the polymer brush SEC traces showed a very minor shift to higher molecular weight upon chain extension with ManAA (DP = 10, BP4). Apparently, the very hydrophilic sugar segment results in a decrease of hydrodynamic volume (Figure 1a,b). The kinetic data also suggests that random copolymers obtain a gradient distribution of ManAA and NIPAM due to the stark difference in reactivity, which resulted in very different properties when compared to their blocky counterparts.

Cloud Point and Hydrodynamic Size Measurements.

After purification, the polymers were analyzed for their cloud points (CP) via UV–vis spectroscopy. Poly(NIPAM) is known for its thermoresponsive solution properties, showing phase separation at around 31–33 °C, depending on the molecular weight and architecture.⁷⁰ The CP of poly(EtOx) was shown to be ~61–65 °C, depending on its chain length.⁷¹ The thermoresponsive behavior of the brush copolymers introduces the possibility to control the solution behavior of the brush copolymers by varying the amount and distribution of NIPAM. This temperature-induced aggregation of the polymers will affect the investigated properties of lectin binding and encapsulation of hydrophobic small molecules.

As expected, the brush-initiator (BI), consisting of 80% EtOx and 20% InOx, exhibited a slightly higher cloud point of around 70 °C. Furthermore, the expected absence of a CP for the brush polymers consisting only of ManAA (BP3, BP4), due to the highly hydrophilic character, was confirmed. Surprising results were obtained for linear and brush copolymers consisting of both NIPAM and/or ManAA.

Depending on the NIPAM ratio and polymer chain sequence (random, block, or reverse block order), the thermoresponsive behavior varied severely (Table 1). Brush polymers consisting of 10 NIPAM units per brush (BP1) showed no thermoresponsive behavior over the measured range, whereas 50 NIPAM units per brush (BP2) exhibited a CP of 35.7 °C. Therefore, a threshold content of NIPAM in the brush polymer is required in order to result in detectable aggregation using the UV–vis method. In general, thermoresponsive properties were not observed for polymers with a 50/50 ratio between NIPAM and ManAA, which is again expected, due to the highly hydrophilic character of the mannose moieties.

The brush copolymer with a random distribution of NIPAM (DP = 50) and ManAA (DP = 10) (BP6) exhibited a CP of 67.5 °C (Figure 2a). Altering the monomer distribution to NIPAM as the first block (DP = 50) and ManAA (DP = 10) as the second block (BP10) gave a minor increase in absorbance around the temperature of the usual CP of poly(NIPAM), where the transmittance dropped to ~90% (Figure 2b). Upon swapping the block sequence of NIPAM and ManAA (BP12), no decrease in transmittance was observed over the measured temperature range.

Interestingly, the sequence of the polymer brushes has a tremendous impact on their solution behaviors. The decrease in transmittance for BP10 can be explained by the hydrophilicity of the flanking sugar blocks, which mediate sufficient solubility for the polymer even though the CP of NIPAM is reached. In the case of a very low sugar ratio (average of one mannose unit per chain, BP7, BP9), the expected results were obtained. The brush polymer with 50 units of NIPAM (BP9) showed a slightly increased CP of 37.5 °C compared to the NIPAM homopolymer (BP2). Surprisingly, BP1, which has a theoretical composition of NIPAM₁₀-*b*-ManAA₁, exhibits a CP at 65.5 °C, although the NIPAM homopolymer (DP = 10) BP1 displays no decrease in transmittance.

According to their cloud points, the particle size of the glyco brush copolymers in water was analyzed by dynamic light scattering (DLS) measurements. In general, polymers with a cloud point below 40 °C formed large aggregates above 35 °C, showing an increase of average size distribution from 19 to 189 nm and 30 to 221 nm for BP2 and BP9, respectively (Table 1). The increase in average size was much smaller for polymers with a NIPAM to ManAA ratio of 50/10. Due to their higher hydrophilic character, the block polymers BP10 and BP12 resulted in an increased particle size from 33 to 74 nm and 25 to 52 nm, respectively. The average size of the random brush copolymer BP6 only increased from 24 to 36 nm (Figure 2). Therefore, the sequence of the brush is demonstrated as an adjustable feature to fine-tune thermoresponsiveness. Generally, brush polymer particle sizes remained unchanged or only increased marginally for higher ratios of ManAA (Figure 3).

Encapsulation Studies with DHA. In order to investigate the drug delivery potential of the synthesized polymer library, aqueous polymer solutions (concentration = 1 mg/mL) were incubated with the hydrophobic compound 1,4-dihydroxyanthraquinone (DHA). DHA was used as an inexpensive, water-insoluble drug mimic to assess the uptake behavior of each polymer for hydrophobic small molecules. Depending on the amount of NIPAM and the polymer architecture, the detected amount of incorporated DHA varied drastically (Figure 4). Generally, the encapsulated amount of DHA in solution increased at elevated temperature (37 °C). The linear

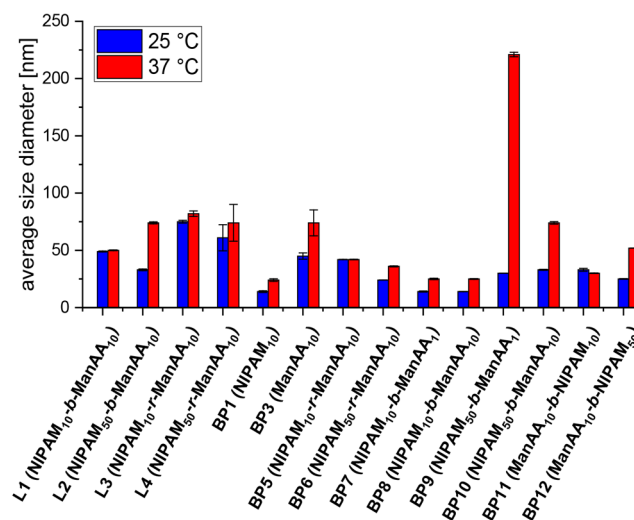


Figure 3. Bar diagram showing the average particle diameter size of an aqueous 1 mg/mL polymer solution at 25 and 37 °C determined by DLS (data are shown as mean + SD).

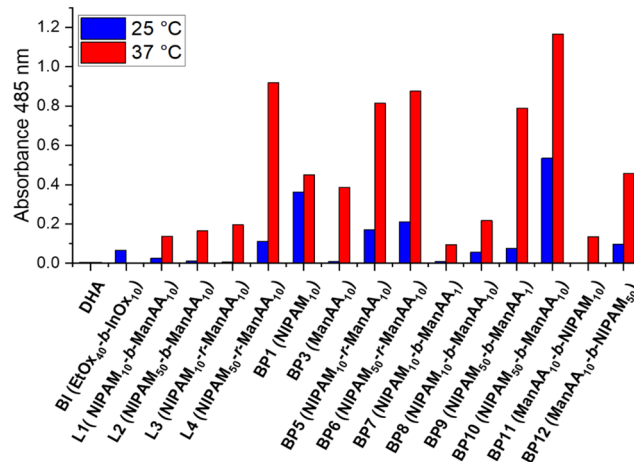


Figure 4. Bar diagram showing the absorbance values at 485 nm of aqueous polymer solutions (1 mg/mL) after incubation with DHA for 12 h at 25 and 37 °C.

polymers L1–L3 showed minor encapsulation, whereas the random copolymer L4 with 50 NIPAM units resulted in a strong increase of DHA uptake compared to the block polymer counterpart L2. However, brush polymers demonstrated contrasting results, showing a higher DHA uptake for block polymer structures (BP8, BP10) over their randomly distributed counterparts (BP5, BP6).

Brush polymers carrying NIPAM at the periphery (B11, B12) encapsulated only a very small amount of the hydrophobic compound. Therefore, the ratio of NIPAM is not crucial for efficient encapsulation of DHA, but the polymer architecture is important. The uptake efficiency is also dependent on the 2-oxazoline backbone. Although showing only a minor response in the UV–vis measurement, the brush initiator (BI) solubilizes a small amount of DHA. More impressively, the highly hydrophilic brush polymer BP3 with 10 mannose units per brush demonstrates a significant increase in DHA encapsulation at 37 °C. The combination of the BI brush initiator backbone with the hydrophilic mannose moieties suggests the establishment of an amphiphilic

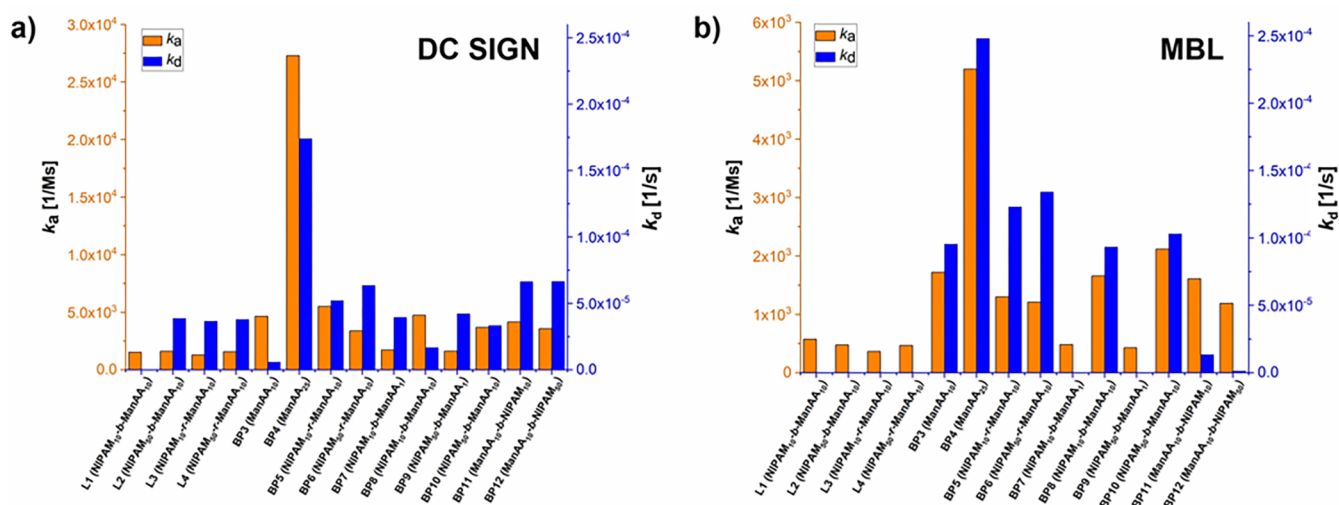


Figure 5. Summary of k_a (orange) and k_d (blue) values for the binding of the glyco brush copolymer library to (a) DC-SIGN and (b) MBL. SPR sensorgrams are presented in Supporting Information (Figure S23–25).

environment, promoting DHA uptake. Consequently, the character of the brush backbone seems to be critical for efficient DHA encapsulation. These preliminary findings provide a promising molecular design for a protein-binding polymer with the ability to deliver a cargo to a specific biological environment. The follow up studies will focus on the uptake measurements with bioactive compounds.

C-Type Lectin Binding Studies via SPR Measurements. The lectin binding behavior of the synthesized polymer library was investigated via SPR measurements. It is important to obtain an in-depth understanding of the interactions between carbohydrate ligands and sugar-binding proteins because this may relate to the biological significance of lectins. The C-type lectins DC-SIGN and MBL were chosen due to their scientific relevance in many biological processes, such as immune response and disease.^{13,72} In general, all polymers carrying mannose units showed some binding, and binding was faster toward DC-SIGN compared to MBL (Figure 5). The absence of lectin binding to NIPAM brush polymers (BP1, BP2) was expected.

Linear polymers showed much slower association kinetics compared to their brush polymer counterparts, which was expected due to the lower sugar density. Remarkably, the linear polymers L1–L4 showed very slow dissociation rates (k_d) for MBL. Similar results were obtained for the binding of L1 to DC-SIGN, although L2–L4 resulted in somewhat increased k_d values (Figure 5). It has to be noted that improved binding (increased R_{max} , Table S1, SI) was observed for the linear block copolymer L1 over the randomly distributed equivalent (L3) for both lectins. This result is in accordance with literature findings, which report better lectin binding for DC-SIGN when the sugar density is high.¹¹ However, linear glycopolymers with NIPAM/ManAA ratios of 50/10 showed very similar binding behavior for linear block and random copolymers (L2 and L4, Figure 6). It is suggested that the hydrophilicity of the polymer chain and the length of the nonbinding segment are pivotal in linear architectures.

On the other hand, glyco brush copolymers showed less pronounced effects of the monomer sequence on lectin binding. As expected, polymers with brushes consisting of only ManAA (BP3, BP4) resulted in very good binding for both lectins, showing increased kinetic values for longer

ManAA segments (BP4) binding DC-SIGN. The association kinetics toward MBL of brush polymers with blocky architectures (BP8, BP10, BP11, BP12) was higher compared to that of polymers with random brush sequences (BP5, BP6). Furthermore, brush polymers with ManAA segments at the periphery (BP8, BP10) resulted in faster binding than polymers with NIPAM blocks flanking the sugary segments (BP11, BP12). This result was expected since the binding epitopes of the polymers are less accessible when blocked by NIPAM segments. Remarkably, this effect was not observed for DC-SIGN. The binding results for DC-SIGN suggest an independence between sequence and binding strength, showing very similar association and dissociation constants for random and blocky architectures. Dissociation rate constants (k_d) are in general very low for glyco brush copolymers with both lectins, indicating that interactions with mannose units on the side chains tend to persist or that rebinding of released mannose units occurs more rapidly than dissociation of the complex during the buffer wash period. The SPR sensorgrams in Figure 6 reveal strong and similar binding characteristics for most glycopolymers to both lectins, dominated by very slow dissociation rates. Overall, we have concluded that an increase in the carbohydrate valency on the side chains is leading to an increase in binding affinity. Polymer brushes with blocky structures bind better to the lectins compared to brushes with randomly distributed monomers. Furthermore, for polymer brushes with a block sequence, the position of the sugar block affects the binding properties according to K_D values. By positioning the carbohydrate blocks in proximity to the brush polymer backbone, lectin binding was decreased due to the binding epitopes being less accessible for the lectins. Hence, BP8 and BP10 present better binding affinity than BP11 and BP12, respectively (Figure S26, SI).

CONCLUSION

In this study, a set of mannose-containing copolymers, covering a wide range of linear and bottle brush polymers, was synthesized via a “grafting from” approach. We have observed that the sequence of the polymer brushes has a large impact on the thermal properties of the polymers in aqueous solution. Furthermore, we have demonstrated that polyacrylamide bottle brush polymers containing NIPAM and ManAA

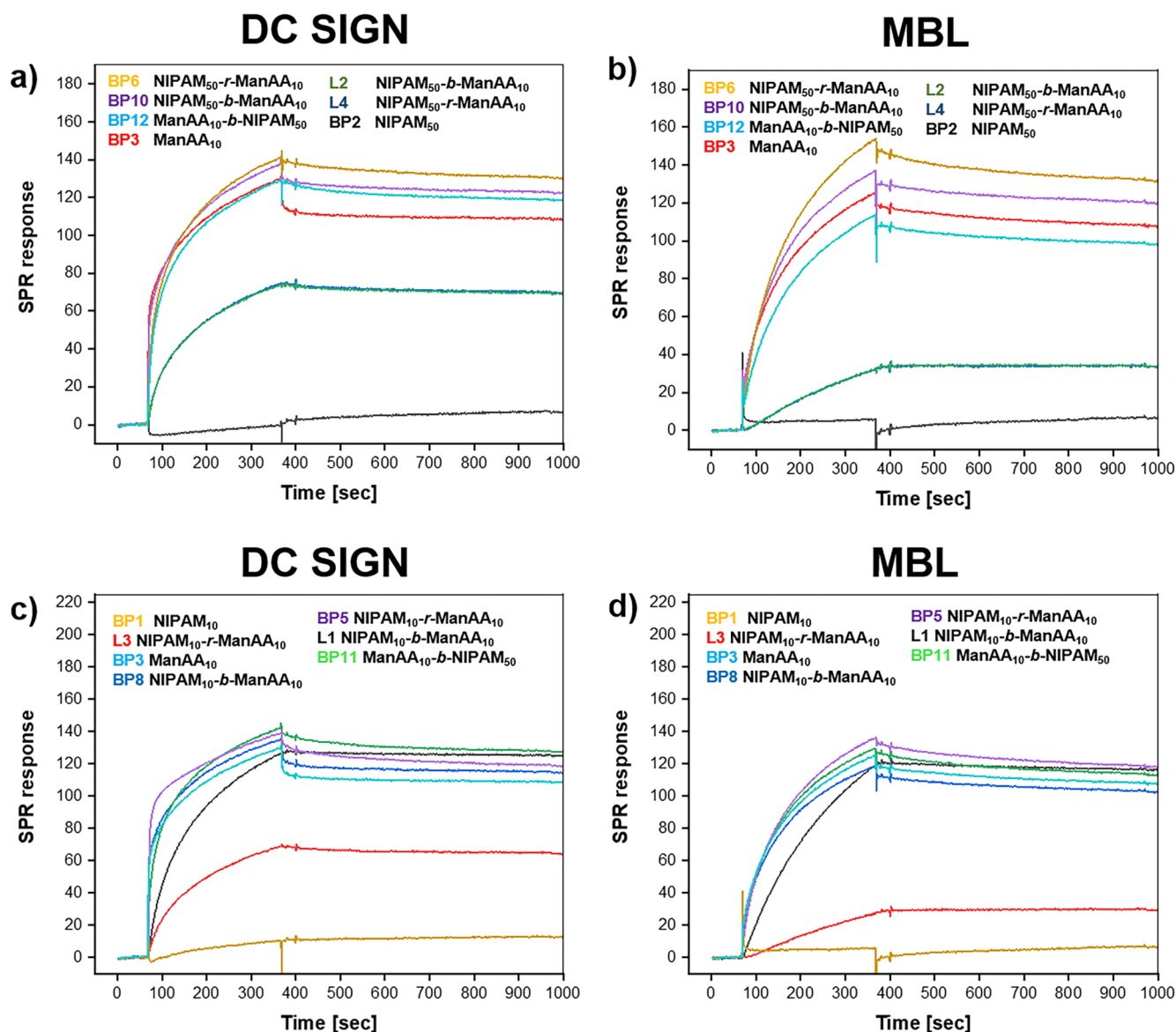


Figure 6. SPR sensorgrams of polymer binding toward MBL and DC-SIGN: (a) DC-SIGN results for polymers with 50 NIPAM units and 10 ManAA units, (b) MBL results for polymers with 50 NIPAM units and 10 ManAA units, (c) DC-SIGN results for polymers with 10 NIPAM units and 10 ManAA units, and (d) MBL results for polymers with 50 NIPAM units and 10 ManAA units.

with a poly(2-oxazoline) backbone show very strong binding to the C-type lectins MBL and DC-SIGN due to the high carbohydrate density and very slow dissociation rates in all cases. The kinetics of the lectin binding assessed via SPR measurements showed accelerated association kinetics of brush architectures compared to their linear counterparts for both lectins. Interestingly, MBL binding association rates depended strongly on the brush sequences, whereas the effects were smaller with DC-SIGN, which showed good binding regardless of the brush constitution. Finally, the integration of a thermoresponsive NIPAM block resulted in an increased incorporation of the drug-mimicking compound DHA, and the cloud point behavior could be tuned by changing monomer ratios and polymer architecture.

■ ASSOCIATED CONTENT

Supporting Information

The Supporting Information is available free of charge at <https://pubs.acs.org/doi/10.1021/acs.biomac.0c00246>.

Sections discussing the materials, methods, and instruments; synthesis and characterization; and lectin binding studies, including Figures S1–S26 and Table S1 (PDF)

■ AUTHOR INFORMATION

Corresponding Author

C. Remzi Becer – Department of Chemistry, University of Warwick, Coventry CV4 7AL, United Kingdom; orcid.org/0000-0003-0968-6662; Email: remzi.becer@warwick.ac.uk

Authors

Valentin P. Beyer – Polymer Chemistry Laboratory, School of Engineering and Materials Science, Queen Mary University of

London, London E1 4NS, United Kingdom; Department of Chemistry, University of Warwick, Coventry CV4 7AL, United Kingdom

Alessandra Monaco – Polymer Chemistry Laboratory, School of Engineering and Materials Science, Queen Mary University of London, London E1 4NS, United Kingdom; Department of Chemistry, University of Warwick, Coventry CV4 7AL, United Kingdom

Richard Napier – School of Life Sciences, University of Warwick, Coventry CV4 7AL, United Kingdom

Gokhan Yilmaz – Department of Chemistry, University of Warwick, Coventry CV4 7AL, United Kingdom

Complete contact information is available at:

<https://pubs.acs.org/10.1021/acs.biomac.0c00246>

Notes

The authors declare no competing financial interest.

LIST OF ABBREVIATIONS

Cu-RDRP, Cu-mediated reversible deactivation radical polymerization; DC-SIGN, dendritic cell-specific intercellular adhesion molecule-3-grabbing nonintegrin; MBL, mannose-binding lectin; HPMA, *N*-(2-hydroxypropyl)methacrylamide; PEG, polyethylene glycol; NIPAM, *N*-isopropylacrylamide; ManAA, 2-(*D*-manosyloxy) hydroxylethylacrylamide; CROP, cationic ring-opening polymerization; BI, brush initiator; DP, degree of polymerization; SEC, size exclusion chromatography; BP, brush polymer; CP, cloud point; DLS, dynamic light scattering; DHA, dihydroxyanthraquinone; SPR, surface plasmon resonance; SD, standard deviation

REFERENCES

- (1) Ghazarian, H.; Idoni, B.; Oppenheimer, S. B. A Glycobiology Review: Carbohydrates, Lectins and Implications in Cancer Therapeutics. *Acta Histochem.* **2011**, *113* (3), 236–247.
- (2) Kerrigan, A. M.; Brown, G. D. C-Type Lectins and Phagocytosis. *Immunobiology* **2009**, *214* (7), 562–575.
- (3) Lundquist, J. J.; Toone, E. J. The Cluster Glycoside Effect. *Chem. Rev.* **2002**, *102* (2), 555–578.
- (4) Burke, S. D.; Zhao, Q.; Schuster, M. C.; Kiessling, L. L. Synergistic Formation of Soluble Lecfin Clusters by a Templated Multivalent Saccharide Ligand. *J. Am. Chem. Soc.* **2000**, *122* (18), 4518–4519.
- (5) Cambi, A.; Koopman, M.; Figdor, C. G. How C-Type Lectins Detect Pathogens. *Cell. Microbiol.* **2005**, *7* (4), 481–488.
- (6) Yamashita, K.; Kuno, A.; Matsuda, A.; Ikehata, Y.; Katada, N.; Hirabayashi, J.; Narimatsu, H.; Watanabe, M. Lectin Microarray Technology Identifies Specific Lectins Related to Lymph Node Metastasis of Advanced Gastric Cancer. *Gastric Cancer* **2016**, *19* (2), 531–542.
- (7) Dube, D. H.; Bertozzi, C. R. Glycans in Cancer and Inflammation - Potential for Therapeutics and Diagnostics. *Nat. Rev. Drug Discovery* **2005**, *4* (6), 477–488.
- (8) Mody, R.; Joshi, S. H. a.; Chaney, W. Use of Lectins as Diagnostic and Therapeutic Tools for Cancer. *J. Pharmacol. Toxicol. Methods* **1995**, *33* (1), 1–10.
- (9) Zhou, R.; Wang, X.; Liu, H.; Guo, L.; Su, Q.; Wang, H.; Vasiliadis, T.; Ho, W.; Li, J. GalNAc-Specific Soybean Lectin Inhibits HIV Infection of Macrophages through Induction of Antiviral Factors. *J. Virol.* **2018**, *92* (6), e01720-17.
- (10) Mazalovska, M.; Koukam, J. C. Lectins as Promising Therapeutics for the Prevention and Treatment of HIV and Other Potential Coinfections. *BioMed Res. Int.* **2018**, *2018*, 1–12.
- (11) Becer, C. R.; Gibson, M. I.; Geng, J.; Ilyas, R.; Wallis, R.; Mitchell, D. A.; Haddleton, D. M. High-Affinity Glycopolymer

Binding to Human DC-SIGN and Disruption of DC-SIGN Interactions with HIV Envelope Glycoprotein. *J. Am. Chem. Soc.* **2010**, *132* (43), 15130–15132.

(12) Zhang, Q.; Collins, J.; Anastasaki, A.; Wallis, R.; Mitchell, D. A.; Becer, C. R.; Haddleton, D. M. Sequence-Controlled Multi-Block Glycopolymers to Inhibit DC-SIGN-GP120 Binding. *Angew. Chem., Int. Ed.* **2013**, *52* (16), 4435–4439.

(13) Turner, M. W. The Role of Mannose-Binding Lectin in Health and Disease. *Mol. Immunol.* **2003**, *40* (7), 423–429.

(14) Saifuddin, M.; Hart, M. L.; Gewurz, H.; Zhang, Y.; Spear, G. T. Interaction of Mannose-Binding Lectin with Primary Isolates of Human Immunodeficiency Virus Type 1. *J. Gen. Virol.* **2000**, *81* (4), 949–955.

(15) Ji, X.; Gewurz, H.; Spear, G. T. Mannose Binding Lectin (MBL) and HIV. *Mol. Immunol.* **2005**, *42*, 145–152.

(16) Svajger, U.; Anderlueh, M.; Jeras, M.; Obermajer, N. C-Type Lectin DC-SIGN: An Adhesion, Signalling and Antigen-Uptake Molecule That Guides Dendritic Cells in Immunity. *Cell. Signalling* **2010**, *22*, 1397–1405.

(17) Kase, T.; Suzuki, Y.; Kawai, T.; Sakamoto, T.; Ohtani, K.; Eda, S.; Maeda, A.; Okuno, Y.; Kurimura, T.; Wakamiya, N. Human Mannan-Binding Lectin Inhibits the Infection of Influenza a Virus without Complement. *Immunology* **1999**, *97* (3), 385–392.

(18) Kurokawa, K.; Takahashi, K.; Lee, B. L. The Staphylococcal Surface-Glycopolymer Wall Teichoic Acid (WTA) Is Crucial for Complement Activation and Immunological Defense against Staphylococcus Aureus Infection. *Immunobiology* **2016**, *221*, 1091–1101.

(19) Michelow, I. C.; Lear, C.; Scully, C.; Prugar, L. I.; Longley, C. B.; Yantosca, L. M.; Ji, X.; Karpel, M.; Brudner, M.; Takahashi, K.; Spear, G. T.; Ezekowitz, R. A. B.; Schmidt, E. V.; Olinger, G. G. High-Dose Mannose-Binding Lectin Therapy for Ebola Virus Infection. *J. Infect. Dis.* **2011**, *203* (2), 175–179.

(20) Kuipers, S.; Aerts, P. C.; Cluysenaer, O. J. J.; Bartelink, A. K. M.; Ezekowitz, R. A. B.; Bax, W. A.; Salimans, M.; Vandyk, H. A Case of Familial Meningococcal Disease Due to Deficiency in Mannose-Binding Lectin (MBL). *Advances in Experimental Medicine and Biology* **2003**, *531*, 351–355.

(21) Garred, P.; Larsen, F.; Madsen, H. O.; Koch, C. Mannose-Binding Lectin Deficiency - Revisited. *Mol. Immunol.* **2003**, *40*, 73–84.

(22) Becer, C. R. The Glycopolymer Code: Synthesis of Glycopolymers and Multivalent Carbohydrate-Lectin Interactions. *Macromol. Rapid Commun.* **2012**, *33* (9), 742–752.

(23) Miura, Y.; Hoshino, Y.; Seto, H. Glycopolymer Nanobiotechnology. *Chem. Rev.* **2016**, *116* (4), 1673–1692.

(24) Ting, S. R. S.; Chen, G.; Stenzel, M. H. Synthesis of Glycopolymers and Their Multivalent Recognitions with Lectins. *Polym. Chem.* **2010**, *1* (9), 1392–1412.

(25) Ponader, D.; Wojcik, F.; Beceren-Braun, F.; Dervedde, J.; Hartmann, L. Sequence-Defined Glycopolymer Segments Presenting Mannose: Synthesis and Lectin Binding Affinity. *Biomacromolecules* **2012**, *13* (6), 1845–1852.

(26) Liu, Z.; Zhu, Y.; Ye, W.; Wu, T.; Miao, D.; Deng, W.; Liu, M. Synthesis of Well-Defined Glycopolymers with Highly Ordered Sugar Units in the Side Chain: Via Combining CuAAC Reaction and ROMP: Lectin Interaction Study in Homo- and Hetero-Glycopolymers. *Polym. Chem.* **2019**, *10* (29), 4006–4016.

(27) Nagao, M.; Kurebayashi, Y.; Seto, H.; Tanaka, T.; Takahashi, T.; Suzuki, T.; Hoshino, Y.; Miura, Y. Synthesis of Well-Controlled Glycopolymers Bearing Oligosaccharides and Their Interactions with Influenza Viruses. *Polym. J.* **2016**, *48* (6), 745–749.

(28) Lavilla, C.; Yilmaz, G.; Uzunova, V.; Napier, R.; Becer, C. R.; Heise, A. Block-Sequence-Specific Glycopolypeptides with Selective Lectin Binding Properties. *Biomacromolecules* **2017**, *18* (6), 1928–1936.

(29) Gou, Y.; Slavin, S.; Geng, J.; Voorhaar, L.; Haddleton, D. M.; Becer, C. R. Controlled Alternate Layer-by-Layer Assembly of Lectins and Glycopolymers Using QCM-D. *ACS Macro Lett.* **2012**, *1* (1), 180–183.

- (30) Jono, K.; Nagao, M.; Oh, T.; Sonoda, S.; Hoshino, Y.; Miura, Y. Controlling the Lectin Recognition of Glycopolymers: Via Distance Arrangement of Sugar Blocks. *Chem. Commun.* **2018**, *54* (1), 82–85.
- (31) Slavin, S.; Burns, J.; Haddleton, D. M.; Becer, C. R. Synthesis of Glycopolymers via Click Reactions. *Eur. Polym. J.* **2011**, *47* (4), 435–446.
- (32) Yilmaz, G.; Uzunova, V.; Napier, R.; Becer, C. R. Single-Chain Glycopolymer Folding via Host-Guest Interactions and Its Unprecedented Effect on DC-SIGN Binding. *Biomacromolecules* **2018**, *19* (7), 3040–3047.
- (33) Yilmaz, G.; Becer, C. R. Glyconanoparticles and Their Interactions with Lectins. *Polym. Chem.* **2015**, *6* (31), 5503–5514.
- (34) Yilmaz, G.; Messenger, L.; Gleinich, A. S.; Mitchell, D. A.; Battaglia, G.; Becer, C. R. Glyconanoparticles with Controlled Morphologies and Their Interactions with a Dendritic Cell Lectin. *Polym. Chem.* **2016**, *7* (41), 6293–6296.
- (35) Li, X.; Chen, G. Glycopolymer-Based Nanoparticles: Synthesis and Application. *Polym. Chem.* **2015**, *6* (9), 1417–1430.
- (36) Kutcherlapati, S. N. R.; Koyilapu, R.; Boddu, U. M. R.; Datta, D.; Perali, R. S.; Swamy, M. J.; Jana, T. Glycopolymer-Grafted Nanoparticles: Synthesis Using RAFT Polymerization and Binding Study with Lectin. *Macromolecules* **2017**, *50* (18), 7309–7320.
- (37) Boden, S.; Wagner, K. G.; Karg, M.; Hartmann, L. Presenting Precision Glycomacromolecules on Gold Nanoparticles for Increased Lectin Binding. *Polymers (Basel, Switz.)* **2017**, *9* (12), 716.
- (38) Basuki, J. S.; Esser, L.; Duong, H. T. T.; Zhang, Q.; Wilson, P.; Whittaker, M. R.; Haddleton, D. M.; Boyer, C.; Davis, T. P. Magnetic Nanoparticles with Diblock Glycopolymer Shells Give Lectin Concentration-Dependent MRI Signals and Selective Cell Uptake. *Chem. Sci.* **2014**, *5* (2), 715–726.
- (39) Serizawa, T.; Yasunaga, S.; Akashi, M. Synthesis and Lectin Recognition of Polystyrene Core-Glycopolymer Corona Nanospheres. *Biomacromolecules* **2001**, *2* (2), 469–475.
- (40) Vandewalle, S.; Wallyn, S.; Chattopadhyay, S.; Becer, C. R.; Du Prez, F. Thermoresponsive Hyperbranched Glycopolymers: Synthesis, Characterization and Lectin Interaction Studies. *Eur. Polym. J.* **2015**, *69*, 490–498.
- (41) Semsarilar, M.; Ladmiraal, V.; Perrier, S. Highly Branched and Hyperbranched Glycopolymers via Reversible Addition-Fragmentation Chain Transfer Polymerization and Click Chemistry. *Macromolecules* **2010**, *43* (3), 1438–1443.
- (42) Zhang, Y.; Wang, B.; Zhang, Y.; Zheng, Y.; Wen, X.; Bai, L.; Wu, Y. Hyperbranched Glycopolymers of 2-(α -D-Mannopyranose) Ethyl Methacrylate and N, N'-Methylenebisacrylamide: Synthesis, Characterization and Multivalent Recognitions with Concanavalin A. *Polymers (Basel, Switz.)* **2018**, *10* (2), 171.
- (43) Lin, K.; Kasko, A. M. Effect of Branching Density on Avidity of Hyperbranched Glycomimetics for Mannose Binding Lectin. *Biomacromolecules* **2013**, *14* (2), 350–357.
- (44) Gormley, A. J.; Yeow, J.; Ng, G.; Conway, Ó.; Boyer, C.; Chapman, R. An Oxygen-Tolerant PET-RAFT Polymerization for Screening Structure–Activity Relationships. *Angew. Chem., Int. Ed.* **2018**, *57* (6), 1557–1562.
- (45) Chen, Y.; Lord, M. S.; Piloni, A.; Stenzel, M. H. Correlation between Molecular Weight and Branch Structure of Glycopolymers Stars and Their Binding to Lectins. *Macromolecules* **2015**, *48* (2), 346–357.
- (46) Nagao, M.; Matsubara, T.; Hoshino, Y.; Sato, T.; Miura, Y. Topological Design of Star Glycopolymers for Controlling the Interaction with the Influenza Virus. *Bioconjugate Chem.* **2019**, *30* (4), 1192–1198.
- (47) Tanaka, J.; Gleinich, A. S.; Zhang, Q.; Whitfield, R.; Kempe, K.; Haddleton, D. M.; Davis, T. P.; Perrier, S.; Mitchell, D. A.; Wilson, P. Specific and Differential Binding of N-Acetylgalactosamine Glycopolymers to the Human Macrophage Galactose Lectin and Asialoglycoprotein Receptor. *Biomacromolecules* **2017**, *18* (5), 1624–1633.
- (48) Cakir, N.; Hizal, G.; Becer, C. R. Supramolecular Glycopolymers with Thermo-Responsive Self-Assembly and Lectin Binding. *Polym. Chem.* **2015**, *6* (37), 6623–6631.
- (49) Zhang, Q.; Su, L.; Collins, J.; Chen, G.; Wallis, R.; Mitchell, D. A.; Haddleton, D. M.; Becer, C. R. Dendritic Cell Lectin-Targeting Sentinel-like Unimolecular Glycoconjugates to Release an Anti-HIV Drug. *J. Am. Chem. Soc.* **2014**, *136* (11), 4325–4332.
- (50) Appelhans, D.; Klajnert-Maculewicz, B.; Janaszewska, A.; Lazniewska, J.; Voit, B. Dendritic Glycopolymers Based on Dendritic Polyamine Scaffolds: View on Their Synthetic Approaches, Characteristics and Potential for Biomedical Applications. *Chem. Soc. Rev.* **2015**, *44* (12), 3968–3996.
- (51) David, A.; Kopečková, P.; Rubinstein, A.; Kopeček, J. Enhanced Biorecognition and Internalization of HPMA Copolymers Containing Multiple or Multivalent Carbohydrate Side-Chains by Human Hepatocarcinoma Cells. *Bioconjugate Chem.* **2001**, *12* (6), 890–899.
- (52) Roy, D.; Ghosh, B.; Song, E. H.; Ratner, D. M.; Stayton, P. S. Polymer-Trimannoside Conjugates via a Combination of RAFT and Thiol-Ene Chemistry. *Polym. Chem.* **2013**, *4* (4), 1153–1160.
- (53) Bojarová, P.; Chytil, P.; Mikulová, B.; Bumba, L.; Konefal, R.; Pelantová, H.; Krejzová, J.; Slámová, K.; Petrásková, L.; Kotrčová, L.; Cvačka, J.; Etrych, T.; Křen, V. Glycan-Decorated HPMA Copolymers as High-Affinity Lectin Ligands. *Polym. Chem.* **2017**, *8* (17), 2647–2658.
- (54) David, A.; Kopečková, P.; Kopeček, J.; Rubinstein, A. The Role of Galactose, Lactose, and Galactose Valency in the Biorecognition of N-(2-Hydroxypropyl)Methacrylamide Copolymers by Human Colon Adenocarcinoma Cells. *Pharm. Res.* **2002**, *19* (8), 1114–1122.
- (55) Tavares, M. R.; Bláhová, M.; Sedláková, L.; Elling, L.; Pelantová, H.; Konefal, R.; Etrych, T.; Křen, V.; Bojarová, P.; Chytil, P. High-Affinity N-(2-Hydroxypropyl)Methacrylamide Copolymers with Tailored N-Acetyllactosamine Presentation Discriminate between Galectins. *Biomacromolecules* **2020**, *21* (2), 641–652.
- (56) Chen, Y.; Chen, G.; Stenzel, M. H. Synthesis and Lectin Recognition of Glyco Star Polymers Prepared by “Clicking” Thiocarbohydrates onto a Reactive Scaffold. *Macromolecules* **2010**, *43* (19), 8109–8114.
- (57) Park, H.; Rosencrantz, R. R.; Elling, L.; Böker, A. Glycopolymer Brushes for Specific Lectin Binding by Controlled Multivalent Presentation of N-Acetyllactosamine Glycan Oligomers. *Macromol. Rapid Commun.* **2015**, *36* (1), 45–54.
- (58) Rosencrantz, R. R.; Nguyen, V. H.; Park, H.; Schulte, C.; Böker, A.; Schnakenberg, U.; Elling, L. Lectin Binding Studies on a Glycopolymer Brush Flow-through Biosensor by Localized Surface Plasmon Resonance. *Anal. Bioanal. Chem.* **2016**, *408* (20), 5633–5640.
- (59) Benetti, E. M.; Divandari, M.; Ramakrishna, S. N.; Morgese, G.; Yan, W.; Trachsel, L. Loops and Cycles at Surfaces: The Unique Properties of Topological Polymer Brushes. *Chem. - Eur. J.* **2017**, *23* (51), 12433–12442.
- (60) Morgese, G.; Verbraeken, B.; Ramakrishna, S. N.; Gombert, Y.; Cavalli, E.; Rosenboom, J. G.; Zenobi-Wong, M.; Spencer, N. D.; Hoogenboom, R.; Benetti, E. M. Chemical Design of Non-Ionic Polymer Brushes as Biointerfaces: Poly(2-Oxazine)s Outperform Both Poly(2-Oxazoline)s and PEG. *Angew. Chem., Int. Ed.* **2018**, *57* (36), 11667–11672.
- (61) Yan, W.; Divandari, M.; Rosenboom, J. G.; Ramakrishna, S. N.; Trachsel, L.; Spencer, N. D.; Morgese, G.; Benetti, E. M. Design and Characterization of Ultrastable, Biopassive and Lubricious Cyclic Poly(2-Alkyl-2-Oxazoline) Brushes. *Polym. Chem.* **2018**, *9* (19), 2580–2589.
- (62) Divandari, M.; Morgese, G.; Trachsel, L.; Romio, M.; Dehghani, E. S.; Rosenboom, J. G.; Paradisi, C.; Zenobi-Wong, M.; Ramakrishna, S. N.; Benetti, E. M. Topology Effects on the Structural and Physicochemical Properties of Polymer Brushes. *Macromolecules* **2017**, *50* (19), 7760–7769.
- (63) Morgese, G.; Trachsel, L.; Romio, M.; Divandari, M.; Ramakrishna, S. N.; Benetti, E. M. Topological Polymer Chemistry Enters Surface Science: Linear versus Cyclic Polymer Brushes. *Angew. Chem., Int. Ed.* **2016**, *55* (50), 15583–15588.

- (64) Konradi, R.; Pidhatika, B.; Mühlebach, A.; Textor, M. Poly-2-Methyl-2-Oxazoline: A Peptide-like Polymer for Protein-Repellent Surfaces. *Langmuir* **2008**, *24* (3), 613–616.
- (65) Pidhatika, B.; Möller, J.; Benetti, E. M.; Konradi, R.; Rakhmatullina, E.; Mühlebach, A.; Zimmermann, R.; Werner, C.; Vogel, V.; Textor, M. The Role of the Interplay between Polymer Architecture and Bacterial Surface Properties on the Microbial Adhesion to Polyoxazoline-Based Ultrathin Films. *Biomaterials* **2010**, *31* (36), 9462–9472.
- (66) Yilmaz, G.; Uzunova, V.; Hartweg, M.; Beyer, V.; Napier, R.; Becer, C. R. The Effect of Linker Length on ConA and DC-SIGN Binding of: S -Glucosyl Functionalized Poly(2-Oxazoline)S. *Polym. Chem.* **2018**, *9* (5), 611–618.
- (67) Kempe, K.; Neuwirth, T.; Czaplewska, J.; Gottschaldt, M.; Hoogenboom, R.; Schubert, U. S. Poly(2-Oxazoline) Glycopolymers with Tunable LCST Behavior. *Polym. Chem.* **2011**, *2* (8), 1737–1743.
- (68) Mees, M. A.; Effenberg, C.; Appelhans, D.; Hoogenboom, R. Sweet Polymers: Poly(2-Ethyl-2-Oxazoline) Glycopolymers by Reductive Amination. *Biomacromolecules* **2016**, *17* (12), 4027–4036.
- (69) Beyer, V. P.; Cattoz, B.; Strong, A.; Schwarz, A.; Becer, C. R. Brush Copolymers from 2-Oxazoline and Acrylic Monomers via an Inimer Approach. *Macromolecules* **2020**, DOI: 10.1021/acs.macromol.0c00243.
- (70) Heskins, M.; Guillet, J. E. Solution Properties of Poly(N-Isopropylacrylamide). *J. Macromol. Sci., Chem.* **1968**, *2* (8), 1441–1455.
- (71) Lin, P.; Clash, C.; Pearce, E. M.; Kwei, T. K.; Aponte, M. A. Solubility and Miscibility of Poly(Ethyl Oxazoline). *J. Polym. Sci., Part B: Polym. Phys.* **1988**, *26* (3), 603–619.
- (72) Van Kooyk, Y.; Geijtenbeek, T. B. H. DC-SIGN: Escape Mechanism for Pathogens. *Nat. Rev. Immunol.* **2003**, *3*, 697–709.